Biophysical Reviews (2023) 15:709–719
https://doi.org/10.1007/s12551-023-01083-4

REVIEW

Label-free fluorescence microscopy: revisiting the opportunities with autofluorescent molecules and harmonic generations as biosensors and biomarkers for quantitative biology

María José García[1,2] · Andrés Kamaid[2] · Leonel Malacrida[1,2]

Received: 4 April 2023 / Accepted: 19 June 2023 / Published online: 26 June 2023

Abstract
Over the past decade, the utilization of advanced fluorescence microscopy technologies has presented numerous opportunities to study or re-investigate autofluorescent molecules and harmonic generation signals as molecular biomarkers and biosensors for in vivo cell and tissue studies. The label-free approaches benefit from the endogenous fluorescent molecules within the cell and take advantage of their spectroscopy properties to address biological questions. Harmonic generation can be used as a tool to identify the occurrence of fibrillar or lipid deposits in tissues, by using second and third-harmonic generation microscopy. Combining autofluorescence with novel techniques and tools such as fluorescence lifetime imaging microscopy (FLIM) and hyperspectral imaging (HSI) with model-free analysis of phasor plots has revolutionized the understanding of molecular processes such as cellular metabolism. These tools provide quantitative information that is often hidden under classical intensity-based microscopy. In this short review, we aim to illustrate how some of these technologies and techniques may enable investigation without the need to add a foreign fluorescence molecule that can modify or affect the results. We address some of the most important autofluorescence molecules and their spectroscopic properties to illustrate the potential of these combined tools. We discuss using them as biomarkers and biosensors and, under the lens of this new technology, identify some of the challenges and potentials for future advances in the field.

Keywords Label-free · Autofluorescence · FLIM · Hyperspectral imaging · Phasor plot · Biosensor

Introduction

Autofluorescence originating from tissues can pose challenges for label-based fluorescence imaging (Rich et al. 2013; Pyon et al. 2019). Strong autofluorescent cells and tissues can complicate fluorescence microscopy by interfering with the signals emitted by the labels being used. However, this drawback presents an invaluable opportunity to investigate cellular processes or identify the presence/accumulation of important biological molecules involved in cell fate determination (Stringari et al. 2011; Aguilar-Arnal et al. 2016). The label-free characteristic of these fluorophores is a highlighted aspect, as it eliminates the need to introduce foreign markers or modify the molecules of interest, which could potentially affect their endogenous function (Croce et al. 2016). Some of these molecules are key in metabolic processes; for others, their increase or decrease implies dysregulation of normal physiology. Some examples are NADH, FAD, retinoic acid, porphyrin, vitamins, or lipids (Richards-Kortum and Sevick-Muraca 1996), see Fig. 1. The autofluorescent molecules within the cell are great candidates to be used as biomarkers or biosensors that can report specific cellular processes or the occurrence of a deleterious event. While a biomarker implies the appearance of a molecule that indicates something is happening (e.g., aging, oxidative stress, or senescence), a biosensor can be a molecule that can report the status of a process, and it can offer a measurement that relates to cellular activity

María José García and Andrés Kamaid equally contribute to the present work.

✉ Leonel Malacrida
lmalacrida@hc.edu.uy

[1] Departamento de Fisiopatología, Hospital de Clínicas, Facultad de Medicina, Universidad de La República, Montevideo, Uruguay

[2] Advanced Bioimaging Unit, Institut Pasteur de Montevideo & Universidad de la República, Montevideo, Uruguay

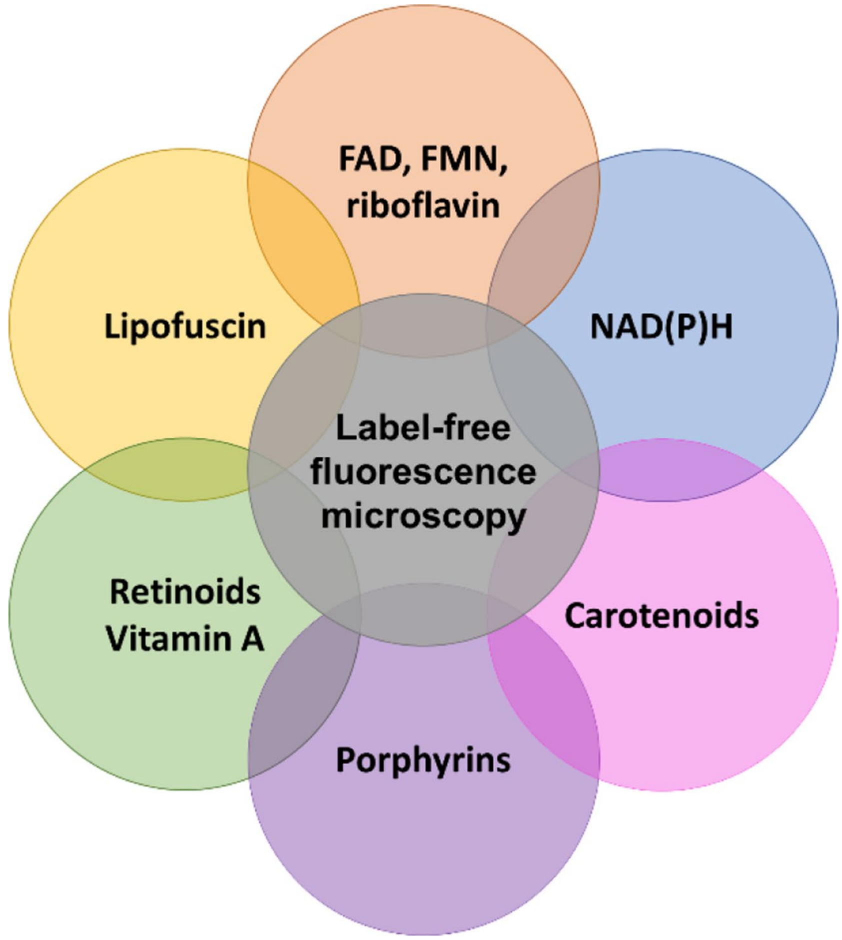

Fig. 1 Autofluorescent molecules in label-free fluorescence microscopy

such as metabolism (Altintas and Tothill 2013; de Oliveira et al. 2020).

The utilization of autofluorescence may pose certain challenges, primarily due to the weak fluorescence exhibited by the target species and their vulnerability to strong bleaching when subjected to single-photon excitation (Klemm et al. 2019). However, these limitations have been successfully overcome through the introduction of multiphoton imaging techniques and the advancements in novel detectors characterized by high quantum yields (Zipfel et al. 2003b; Aptel et al. 2010).

The fluorescence spectrum and lifetime are molecular features that identify a molecule's existence and its status (Ranjit et al. 2018). Due to their broad excitation and emission, autofluorescence for individual markers is difficult to isolate from each other. Thus, it is simpler to handle this data using spectroscopy tools such as time-resolved or spectral imaging (Croce 2021). In the last decade, technologies such as fluorescence lifetime imaging microscopy (FLIM) and hyperspectral imaging (HSI) in combination with multiphoton excitation opened multiple possibilities to address autofluorescence for several life science and biomedical research applications (Hiraoka et al. 2002; Zimmermann et al. 2003; Alfonso-Garcia et al. 2020; Datta et al. 2020). FLIM can be acquired using cameras or scanning-based instruments (Chen et al. 2015; Ranjit et al. 2018). Two main approaches exist to obtain FLIM data, namely the time-domain and frequency-domain. Time-domain relies on fast cards to acquire the fluorescence decay with picosecond resolution (Malacrida et al. 2021). Frequency-domain uses a modulated source of light and simpler electronics to measure the delta phase as indicative of the delay by the fluorescence lifetime of the molecule of interest (Malacrida et al. 2021). HSI instrumentation combines a dispersive optical element to open the fluorescence in a range that can be recorded using an array detector or camera (Zimmermann et al. 2003). A detailed discussion of FLIM and HSI instrumentation and techniques can be found elsewhere (Torrado et al. 2022; Díaz and Malacrida 2023), see Fig. 2.

Classical methods to measure the fluorescence lifetime of autofluorescence through imaging (by FLIM) require knowledge of individual molecules' lifetime fingerprints. Such information must be used to propose fitting models that determine each contributor's lifetime and molecular fraction (Becker 2012). However, there are multiple situations where it is difficult to know a priori the physical model underlining

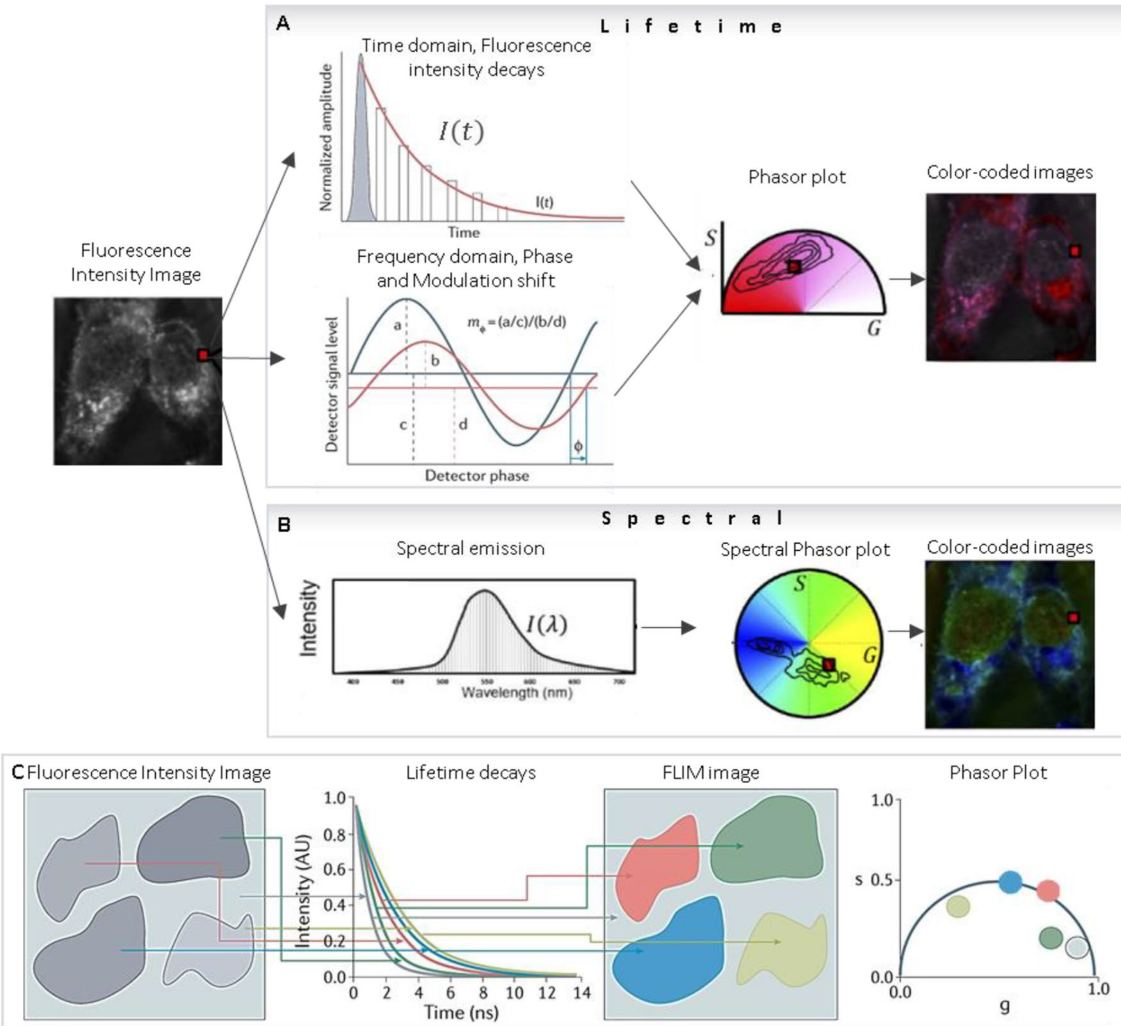

Fig. 2 Fluorescence lifetime imaging microscopy (FLIM) and hyperspectral imaging (HSI) and its analysis by the phasor approach. **A** Fluorescence lifetime imaging microscopy (FLIM), data can be acquired using time or frequency domain (top and bottom, respectively). Using these approaches, it is possible to obtain the average lifetime of a fluorophore. Traditional further analyses involve fitting the decays using single or multiexponential decays. However, the decay or delta phase can be converted into the phasor plot (Fourier transformation). The shorter the modulation vector, the longer the associated lifetime, while an increase in the phase delay indicates an increasing lifetime. For any single exponential decay (single lifetime), the position expected will fall on the universal circle (semi-circle with radius 0.5 unit, and centered at (0.5, 0)). **B** Spectral imaging collects the spectrum pixel-by-pixel. Traditional HSI data is analyzed using different spectral unmixing, and the spectral phasor plot enables one to analyze the data using a model-free approach. The phase shift of the spectral phasor generates the color-coded image. In the spectral phasor plot, the position at the phasor relies on the spectral maximum and bandwidth. Bluer spectra appear at shorter phases from position (1,0) and broader spectra are closer to the center. **C** Using the reciprocity principle for the FLIM-Phasor plot it is possible to identify a region of interest at the phasor plot (selection cursors at phasor plot, right) and color these pixels in the original image generating a FLIM image (central image). This property is shared with the spectral phasor plot. Figure modified from (Torrado et al. 2022)

a process in cells. This kind of situation would benefit from using a model-free approach. The phasor approach for FLIM and HSI data is a model-free approach used for time-resolved and spectral data analysis in which the zeta dimension is converted into the phasor plot by the Fourier transform, see Fig. 2 (Ranjit et al. 2018; Torrado et al. 2022). Using such an approach, it is simple to determine whether a lifetime decay relates to a single exponential decay or it is a combination of n-components (Torrado et al. 2022). Besides being a model-free approach, the phasor plots have valuable properties, such as the linear combination or reciprocity principle that enables one to quantify the fraction of components solving the linear algebra of the linear combination while generating a map of molecular markers in a pseudocolor image by the selection of a region of interest at the phasor plot (Díaz and Malacrida 2023). Taking advantage of these unique properties, many applications of label-free fluorescence microscopy are flourishing (Skala et al. 2007;

Stringari et al. 2011; Dvornikov et al. 2019; Ranjit et al. 2019b). In addition, a group of other label-free approaches uses non-linear microscopy, known as harmonic generation (second and third). These methods enable, for example, the identification of the occurrence of fibers or lipidic deposition in tissues or cells through a non-fluorescent process (Friedl et al. 2007). Such an approach is expanding from basic research to diagnostic and clinical applications (Aptel et al. 2010; Ranjit et al. 2016a, 2017; Ung et al. 2021).

One of the most highlighted examples of label-free microscopy in combination with the phasor plot is the single-cell metabolic fingerprint based on NADH fluorescence (Stringari et al. 2011; Ranjit et al. 2019b; Datta et al. 2020). When NADH binds to enzymes, its fluorescence lifetime changes, so by using these lifetime changes, it is possible to generate a metabolic index that informs about the cellular metabolic fate (glycolysis or oxidative phosphorylation) (Aguilar-Arnal et al. 2016; Ranjit et al. 2019b). Therefore, NADH is an excellent example of an autofluorescent molecule that can be considered as a biosensor.

On the other hand, lipofuscin is an example of an autofluorescent intracellular entity considered a biomarker of aging and senescence (Seehafer and Pearce 2006). In this case, advanced imaging technologies, such as FLIM, have allowed the identification of heterogeneity in lipofuscin's fluorescence lifetime. This result has opened a new research area aimed at understanding its biological meaning and its use as a biosensor.

This short review aims to provide an overview of the most significant autofluorescent molecules and label-free approaches. The focus is on their integration with cutting-edge imaging technologies and tools, allowing for the identification of more accurate and robust biomarkers and biosensors in the realm of quantitative life science research. The advantage of these methods lies in their ability to analyze natural systems without the need for introducing foreign markers that may alter the system under study.

NAD(P)H and FAD as fluorescent metabolic cofactors

Reduced nicotinamide adenine dinucleotide (NADH) and flavin adenine dinucleotide (FAD) are autofluorescent cellular redox cofactors with a central role in energy production (Stringari et al. 2017). Their use as biosensors of metabolic changes relates to Britton Chance's pioneer work in the mid-fifties (Williams and Chance 1955). Since then, many studies have confirmed them as reliable indicators of metabolic activities and mitochondrial functionality (Chance et al. 1962; Zipfel et al. 2003a; DeBerardinis et al. 2008). These molecules can be excited by UV/visible light and 2P excitation, which opens the opportunity for in vivo imaging using multiphoton microscopy (Heikal 2010; Stringari et al. 2017; Kalinina et al. 2021). Measuring their autofluorescence properties offers the opportunity to eliminate toxicity from exogenous fluorophores that may affect cell metabolism, and in fact, novel technologies such as 2P-FLIM or HSI have opened the possibility of understanding metabolic dynamics in basic research and diagnostics for clinical applications (Gosnell et al. 2016; Ranjit et al. 2019b; Kalinina et al. 2021).

Multiphoton microscopy has recently become a powerful metabolic imaging tool (Zipfel et al. 2003b; Skala et al. 2007; Datta et al. 2016; Ranjit et al. 2017). Pulsed near-infrared excitation allows deep imaging of cells and tissues using NAD(P)H and FAD autofluorescence (Stringari et al. 2017; Kalinina et al. 2021). Pulsed light as 2P lasers can be combined to study fluorescence lifetime, providing a molecular fingerprint of molecules and their physical state or interactions (Ma et al. 2016; Ranjit et al. 2019b; Datta et al. 2020). The lifetime of NAD(P)H and FAD changes upon binding to proteins/enzymes (Stringari et al. 2011, 2012). NAD(P)H's fluorescence lifetime is around 0.4 ns for the free version and 2–9 ns for the bound population, depending on the dehydrogenase bound (e.g., 3.4 ns for lactate dehydrogenase) (Ma et al. 2016). This change in the fluorescence lifetime can be exploited to study the cellular metabolic state (Ranjit et al. 2019b; Ung et al. 2021), producing a metabolic index. The metabolic index can be correlated to oxidative phosphorylation (OXPHOS) or glycolysis status as the bound-NADH or free-NADH fractions increase, respectively. FAD also changes fluorescence lifetime for its free or protein-bound fraction (Skala et al. 2007; Stringari et al. 2017; Kalinina et al. 2021; Ung et al. 2021). However, the shorter lifetime is associated with the bound status and the long lifetime of the free FAD (Kalinina et al. 2021). The metabolic index for FAD is less explored, and several reasons make it a more complex problem than NADH. For instance, other flavins, such as riboflavin or flavin mononucleotide (FMN), are fluorescent and can bind to the same protein/enzymes as FAD (Kalinina et al. 2021). Nonetheless, some groups are pushing on the valuable information of free and bound FAD as a biosensor for metabolic studies (Skala et al. 2007; Fereidouni et al. 2014; Ung et al. 2021). On the other hand, either stationary or time-resolved data on images of NADH and FAD have been used over the past decade as an optical redox ratio (ORR) to assess the overall redox state in cells and organs (Skala et al. 2007; Ostrander et al. 2010). In the HSI application for metabolic imaging, new approaches such as the combination of phasor plot and light-sheet microscopy enable quantifying the metabolic status in tissue, opening a new dimension for spatio-temporal studies in animals and embryos (Hedde et al. 2021).

Alterations that can lead to a switch between oxidative phosphorylation and a glycolytic profile are related to the development of cancer and other diseases such as diabetes, neurodegenerative, and cardiovascular disorders (Heikal 2010; Liu et al. 2018). Bioimaging technologies are able to discern spatial and temporal aspects of cells at the microscopic level and thus have an inherent advantage over methods such as magnetic resonance imaging or mass spectroscopy which look at larger (average) targets.

Porphyrins autofluorescence and its use in neurosurgery

One of the most studied porphyrins is protoporphyrin IX (PPIX). It is a product of the heme biosynthetic pathway, and its organic structure relies on four pyrrole rings (Sachar et al. 2016). PPIX fluorescence has gained increasing attention for its use in guided neurosurgery. The procedure needs the administration of an exogenous fluorophore precursor, 5-aminolevulinic acid (5-ALA), taken up by glioma cells but not normal brain tissue (DSouza et al. 2016). That preferential selection is because the blood–brain barrier break occurred in areas such as glioma regions.

Porphyrin fluorescence occurs over the range from 600 to 730 nm, using 415 nm excitation light. Due to the broad porphyrin emission, a strong overlap is found with other autofluorescence molecules. Several strategies have been used to quantify the relative contribution of the different components. For instance, using single excitation with UV light and two bandpass filters (590–800 porphyrin fluorescence and 520–560 autofluorescence) can be used to discriminate between porphyrin and other autofluorescence (Lu et al. 2020). Nonetheless, it is possible to access molecular information of the PPIX lifetime using time-resolved imaging to avoid problems with other autofluorescence present in the tissue or light scattering (Erkkilä et al. 2019). This approach has demonstrated enhanced sensitivity for fluorescence-guided neurosurgery.

Moreover, the lifetime dimension has opened other possibilities, such as characterizing specific tumor variants on the lifetime of PPIX (Reichert et al. 2021). For instance, this approach of lifetime fluorescence imaging of low-grade glioma, high-grade glioma, meningioma, and metastases was compared, measuring the lifetime of PPIX and NADH. Significant changes in lifetimes among the different tumors are evident (infiltration zones 4.1 ns, high-grade glioma and metastasis around 4.8 ns, and meningioma tumor ~ 12.2 ns). This difference in various tumors was then confirmed as bi-exponential behavior with lifetimes of 2 and 16 ns using the model-free phasor approach (Erkkilä et al. 2020).

Hence, PPIX lifetime-based fluorescence measurements show the potential of these tools for clinical approaches in supporting neurosurgeons' decisions in the surgery room.

Vitamin A and retinoid-related autofluorescence molecules

Retinoids comprise a diverse family of organic compounds derived from vitamin A that plays a central role in animal physiology. They exert their function primarily by modulating transcriptional control in the cell nucleus to regulate various cellular processes, including cell differentiation, proliferation, apoptosis, and others. Not surprisingly, the deregulation of retinoid signaling pathways has been linked to several diseases, such as embryonic teratogenesis and tumorigenesis (Petkovich and Chambon 2022). Vitamin A shows a characteristic yellowish-greenish autofluorescence in the porcine embryo using a 330–385 nm excitation filter (Schweigert et al. 2002). However, intensity-based measurements are limited due to the similar steady-state spectroscopic profile of vitamin A and retinoid-related molecules. Using 2P excitation (790 nm), FLIM-phasor analysis showed that retinol and retinoic acid in DMSO displayed distinct locations at the phasor plot. Both were multiexponential decay due to their location inside the universal circle, but with retinoic acid close to position (0,0), meaning a short lifetime, and retinol with a longer lifetime close to 3 ns (Stringari et al. 2011).

Interestingly, endogenous retinoic acid has been measured in vivo during embryonic brain development. In a recent study, 2P-FLIM-phasor analysis was used to investigate the noise amplitude in retinoic acid signaling in specific hindbrain segments of zebrafish embryos (Sosnik et al. 2016). This study showed how this robust and precise approach can tackle important embryogenesis questions.

Lipid-related biosensors/biomarkers

Carotenoids in ophthalmoscopy diagnosis

The most predominant carotenoids in the retina are lutein and zeaxanthin, mainly located at the macular center. Carotenoids are responsible for the yellowish color of the fovea. Its absorbance at 460 nm is a blue filter for UV light (Barker et al. 2011). The broad fluorescence of both compounds is weak around 550 nm when excited at 473 nm, with a lifetime range of 41 and 84 ps (Dysli et al. 2017). Nevertheless, when zeaxanthin forms aggregates, its lifetimes increase to 1.06 ns with a maximum emission at 680 nm (Gruszecki et al. 1990). Fluorescence lifetime imaging ophthalmoscopy (FLIO) has taken advantage of macular pigment (MP) to analyze carotenoids' ex vivo fluorescence characteristics. FLIO appears to be a valuable tool for the early diagnosis of various retinal diseases (Sauer et al. 2018).

Lipofuscin as an aging autofluorescence biomarker

Lipofuscin (LF) is the name given to an intracellular entity that forms endogenously in different post-mitotic animal cell types, initially observed using transmitted light-microscopy and described as a yellow–brown pigment that has also been named lipopigment or chromolipid (Sohal and Wolfe 1986). LF presence has been long considered a hallmark (biomarker) of aging (Sohal and Wolfe 1986; Terman and Brunk 2004) and is currently one of the most widely accepted biomarkers of cellular senescence (Rizou et al. 2019). Many histochemical methods have been used to detect its presence, including some classical lipid-staining techniques and agents, such as Sudan black, Nile and Berlin blue, ferric ferricyanide, hematoxylin and eosin, or osmic acid (Seehafer and Pearce 2006; Jung et al. 2007). However, in later years, LP fluorescence and spectroscopic properties have been used to analyze the chemical composition and physicochemical properties of LF aggregates through microscopy (Terman and Brunk 2004; Jung et al. 2007). LF can be excited with broad UV–VIS laser lines in confocal fluorescence microscopy, and it fluoresces with a spectrum covering 570–605 nm (Jung et al. 2009; Croce et al. 2016). LF can also be excited using 2P-microscopy at 1060 nm, with detection ranging from 604–679 nm (Yan et al. 2023). Combining 2P excitation with FLIM, LF autofluorescence has been shown to discriminate between necrosis and apoptosis with single-cell resolution (Yan et al. 2023). Several results have suggested heterogeneity in LF spectral properties (Marmorstein et al. 2002; Warburton et al. 2007; Yakovleva et al. 2020). The spectral shape and amplitude of the fluorescent signal have been shown to depend on its composition variability (e.g., proteins, lipids, carotenoids), the number of crosslinks, the degree of oxidation of these heterogeneous compounds as well as the concentration of Lipofuscin itself (Terman and Brunk 2004). LF-granules can be identified with age in the retinal pigment epithelium (RPE), particularly in people with progressive age-related macular degeneration (AMD). It is believed that bisretinoids and some photooxidation or photodegradation products are responsible for producing LF-granule fluorescence, illustrating its composition and spectra heterogeneity (Yakovleva et al. 2020). Phasor analysis of LF autofluorescence in the Alzheimer's mouse model shows heterogenic lifetime distribution and a different linear combination with the wild-type mice (Gómez 2018).

Autofluorescent proteins and second harmonic generation (SHG)

Besides fluorescent amino acids, there is a small list of intrinsically fluorescent proteins (elastin, collagen, among others) (Zipfel et al. 2003b; Ranjit et al. 2015). The pyridolamine crosslinks found in elastin and some collagens were shown to be the intrinsic fluorophores responsible for the autofluorescence (Zipfel et al. 2003a). The characteristic elastin ring is found directly beneath the lining of endothelial cells. Sixty percent of the amino acids in elastin are nonpolar, with pyridinoline groups attached to lysine residues (Bridges et al. 1966). These pyridinoline groups are responsible for revealing elastin upon two-photon microscopy as they exhibit an emission maximum at 400 nm when excited with UV light (Bridges et al. 1966; Richards-Kortum and Sevick-Muraca 1996; Zipfel et al. 2003a). Collagens (I, II, III, IV, and V) are one of the main components of the extracellular matrix (ECM) in tissues. All collagens are autofluorescence under 2P-FLIM (Ranjit et al. 2015). Using the phasor plot analysis makes it possible to identify the specific lifetime signatures for each of them and to study different pathologies (Ranjit et al. 2015; Dvornikov et al. 2019). Various diseases are associated with the presence of fibrosis. For instance, liver cirrhosis, idiopathic pulmonary fibrosis, diabetic nephropathy, arteriosclerosis, scleroderma, rheumatoid arthritis, and fibrosarcomas (Raub et al. 2007; Ranjit et al. 2015, 2016a, b). The ratio of collagen III to collagen I show relevance for diagnosing dilated cardiomyopathy (Ranjit et al. 2015). Using 2P-FLIM and phasor analysis greatly simplifies the measurement of collagen III to collagen I (see Fig. 3). Our group has contributed to extending this approach to HSI, using wavelength-modulated filters (sine/cosine transmission) to obtain the spectral phasor signature for collagen III and collagen I. This straightforward and powerful approach can be exploited as a biomarker of these two molecules (Dvornikov et al. 2019).

On the other hand, fibers of different collagens can be identified by a signal known as second harmonic generation (SHG) (Zipfel et al. 2003a; Campagnola 2011; Campagnola and Dong 2011). SHG is a non-linear optical process that occurs when the light of wavelength λ interacts with a non-centrosymmetric fibrillar structure (e.g., collagen I) and produces a signal of half the incident wavelength (λ/2) (Friedl et al. 2007). Among collagens, I and II have the strongest SHG signals, while collagen III gives relatively weak SHG signals (Campagnola and Dong 2011). SHG generation is the most widely used technique for label-free imaging of collagens, allowing one to obtain collagen fingerprints that are then used to identify the presence or absence of fibrosis. Elastin and collagen are thus primary extracellular sources of intrinsic non-linear emissions (Plotnikov et al. 2008; Nadiarnykh et al. 2009; Crosignani et al. 2013; Ranjit et al. 2015). There is increasing literature on the anatomopathological application of SHG in diverse fields such as oncology, nephrology, or ophthalmology.

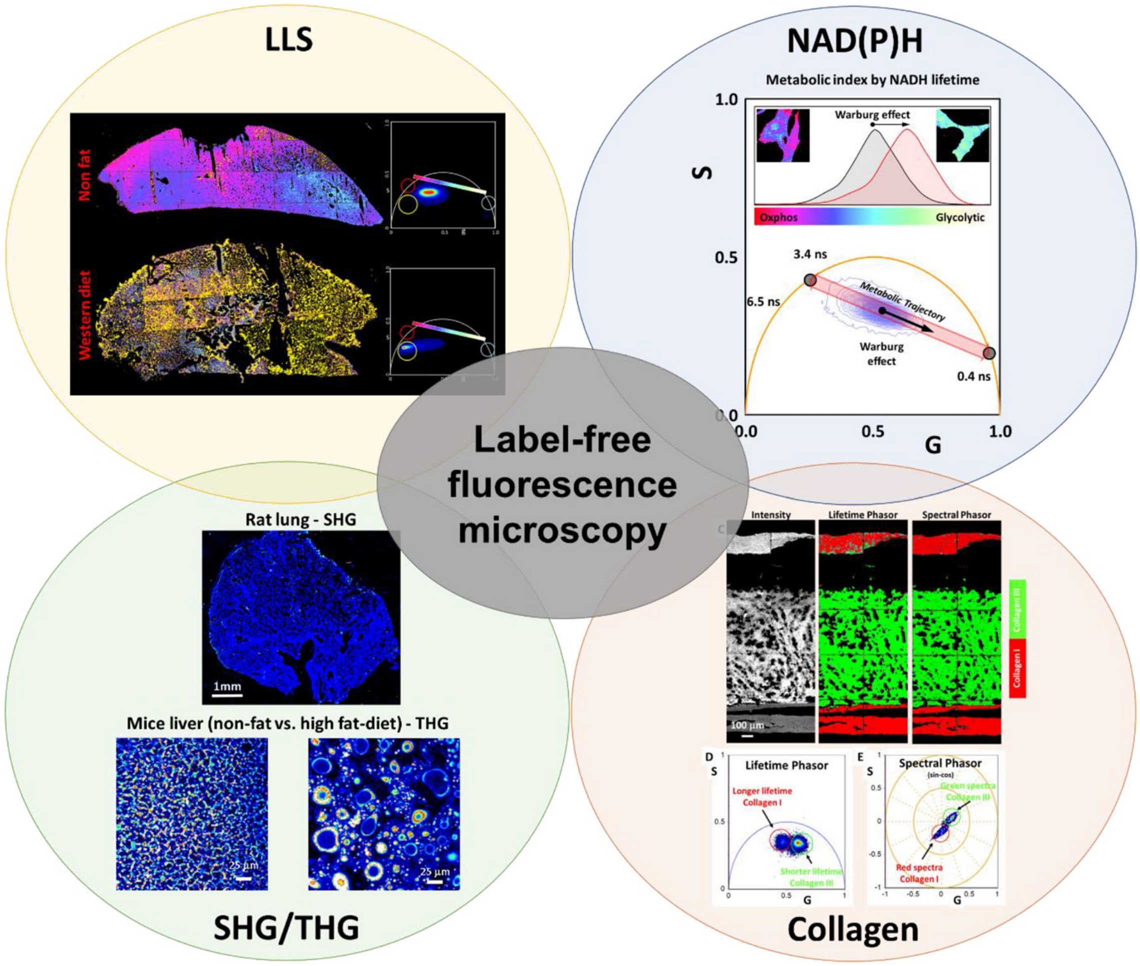

Fig. 3 Examples of autofluorescence used as biomarkers and biosensors. LLS occurrence in mice liver after western diet. Modified from (Ranjit et al. 2017). NAD(P)H and the metabolic index generated by the free and bound NADH trajectory in the phasor plot. The Warburg effect can be identified as the glycolytic shift (white colors). Modified from (Ranjit et al. 2019b). SHG and THG are from rat lungs or mice livers, respectively. Modified from (Dvornikov et al. 2019). FLIM and spectral imaging revealed collagen I and collagen III fluorescence differences. Modified from (Dvornikov et al. 2019)

Third harmonic generation (THG) for lipid deposit studies

Third harmonic generation (THG) occurs at structural interfaces due to abrupt changes in the refractive index (Weigelin et al. 2016). For example, THG occurs on interfaces between interstitial aqueous fluids and lipid-rich structures such as cell membranes (Aptel et al. 2010) and lipid droplets (Débarre et al. 2006; Tserevelakis et al. 2014; Ranjit et al. 2017). In this case, the generated signal is at one-third of the incident wavelength (λ/3). As in the case of SHG, it is essential to clarify that THG and SHG do not imply light absorption. Therefore, time-resolved harmonic generation measurements produce a zero lifetime in FLIM (Dvornikov et al. 2019). THG has been used to study lipid deposits in the liver or other organelles in pathology models, such as high-fat diets in mice (Débarre et al. 2006; Tserevelakis et al. 2014; Ranjit et al. 2017). THG, combined with fluorescence and SHG, makes it possible to visualize essential details of the extracellular matrix, cell morphology, and subcellular organization to identify pathologies related to fat accumulation (Weigelin et al. 2016; Stringari et al. 2017).

Long-lifetime species (LLS) in lipid oxidation and oxidative stress identification

Long lifetime species (LLS) refers to a fluorescence signal originally observed in metabolic FLIM imaging during NADH FLIM analysis using the phasor approach (Datta et al. 2015). The LLS was discovered in cells under oxidative stress and then observed in the livers of mice fed with a high-fat diet (Datta et al. 2015; Ranjit et al. 2017). This fluorescence component was found in the phasor plot analysis of the NADH fluorescence lifetime quantification (Datta et al.

2015; Ranjit et al. 2019a). Note that the model-free phasor approach allowed investigators to identify a long-lifetime component that was not known a priori. While the specific molecular entity responsible for the LLS fluorescence is unclear, using coherent anti-stokes Raman scattering microscopy (CARS), the LLS was assigned to lipids within lipid droplets in the cell (Datta et al. 2015). Different protocols, both in vitro or in vivo, enabled them to be correlated with oxidative stress (Datta et al. 2016; Ranjit et al. 2017). Using the linear combination rules of phasor plots, ones can quantify the fraction of the LLS at the same time as the free and bound NADH fraction, permitting it to become a promising biomarker for cells and in vivo oxidative stress.

Conclusion and remarkable

Technology progress enables us to look at autofluorescence under new lenses with the possibility of opening novel approaches to use them as biomarkers or biosensors. NADH is perhaps one of the most significant autofluorescent molecules used to understand metabolism in vivo; however, flavins, another group of autofluorescent molecules also involved in metabolic process within the cell, can also offer a deeper understanding of the cellular changes that accompany OXPHOS/glycolysis. On the other hand, lipofuscin, retinoic acid, porphyrins, and carotenoids, considered as “classical biomarkers,” may open the possibility, using the new approaches to FLIM and HSI, to identify different states or interactions of these molecules with third components. Label- and model-free approaches are key to identify novel species that were not conceived to exist a priori. Discovery of LLS were hidden under traditional fitting approaches; however, the use of phasor analysis transforms them as an important endogenous biomarker of oxidative stress. The combination of 2P-FLIM and harmonic generation approaches, facilitated by their shared instrumentation, presents an intriguing avenue for exploring biological processes in their natural state and in vivo. This development holds great potential, particularly in fields like developmental biology and embryology, offering unprecedented opportunities for research and investigation. Mini2P microscope for multiphoton microscopy on freely moving mice is compelling example of the next steps in advancing the combination with FLIM and HSI. The integration of these tool holds tremendous potential to elevate our understanding and exploration of autofluorescence to the next level (Zong et al. 2017, 2022). Furthermore, the advent of new tools such as 3-photon microscopy and adaptive optics holds great promise for expanding the excitation bandwidth, enabling sharper and deeper imaging in challenging tissues like the visual cortex or brain (Yildirim et al. 2019; Leemans et al. 2020; Akbari et al. 2022). These cutting-edge technologies open new frontiers in the field of imaging, allowing researchers to delve into previously inaccessible depths and achieve higher resolution in their investigations of complex neural structures.

Overall, we are convinced that advanced microscopy combined with autofluorescence (label-free) will broadly impact life sciences and biomedical diagnostics for the following decades.

Author contribution MJG, AK, and LM write the article. LM conceived and revised the final document.

Funding LM is supported by the grants 2020–225439, 2021–240122, and 2022–252604 of Chan Zuckerberg Initiative DAF, an advised fund of the Silicon Valley Community Foundation. MJG is supported as a PhD student by the Comisión Academica de Posgrado, Comisión Sectorial de Investigación Científica (CSIC), Universidad de la República, Uruguay. LM, AK, and MJG were supported by FOCEM—Fondo para la Convergencia Estructural del Mercosur (COF 03/11).

Declarations

Ethical approval Not applicable.

Consent to participate Not applicable.

Consent for publication Not applicable.

Conflict of interest The authors declare no competing interests.

References

Aguilar-Arnal L, Ranjit S, Stringari C et al (2016) Spatial dynamics of SIRT1 and the subnuclear distribution of NADH species. Proc Natl Acad Sci U S A 113:12715–12720. https://doi.org/10.1073/pnas.1609227113

Akbari N, Tatarsky RL, Kolkman KE et al (2022) Whole-brain optical access in a small adult vertebrate with two- and three-photon microscopy. iScience 25:105191. https://doi.org/10.1016/j.isci.2022.105191

Altintas Z, Tothill I (2013) Biomarkers and biosensors for the early diagnosis of lung cancer. Sensors Actuators, B Chem 188:988–998. https://doi.org/10.1016/j.snb.2013.07.078

Aptel F, Olivier N, Deniset-Besseau A et al (2010) Multimodal nonlinear imaging of the human cornea. Investig Ophthalmol vis Sci 51:2459–2465. https://doi.org/10.1167/iovs.09-4586

Barker FM, Snodderly DM, Johnson EJ et al (2011) Nutritional manipulation of primate retinas, V: effects of lutein, zeaxanthin, and n-3 fatty acids on retinal sensitivity to blue-light-induced damage. Investig Ophthalmol vis Sci 52:3934–3942. https://doi.org/10.1167/iovs.10-5898

Becker W (2012) Fluorescence lifetime imaging – techniques and applications. J Microsc 247:119–136. https://doi.org/10.1111/j.1365-2818.2012.03618.x

Bridges JW, Davies DS, Williams RT (1966) Fluorescence studies on some hydroxypyridines including compounds of the vitamin B6 group. Biochem J 98:451–468. https://doi.org/10.1042/bj0980451

Campagnola P (2011) Second harmonic generation imaging microscopy: applications to diseases diagnostics. Anal Chem 83:3224–3231. https://doi.org/10.1021/ac1032325.Second

Campagnola PJ, Dong CY (2011) Second harmonic generation microscopy: principles and applications to disease diagnosis. Laser Photonics Rev 5:13–26. https://doi.org/10.1002/lpor.200910024
Chance B, Cohen P, Jobsis F, Schoen B (1962) Intracellular Oxidatior Reduction States in ViI O 137:499–508
Chen H, Holst G, Gratton E (2015) Modulated CMOS camera for fluorescence lifetime microscopy. Microsc Res Tech 78:1075–1081. https://doi.org/10.1002/jemt.22587
Croce AC, Ferrigno A, Di Pasqua LG et al (2016) Autofluorescence discrimination of metabolic fingerprint in nutritional and genetic fatty liver models. J Photochem Photobiol B Biol 164:13–20. https://doi.org/10.1016/j.jphotobiol.2016.09.015
Crosignani V, Dvornikov A, Gratton E (2013) Ultra-deep imaging of turbid samples by enhanced photon harvesting. Multiphot Microsc Biomed Sci XIII:8588–858810. https://doi.org/10.1117/12.2002101
Datta R, Alfonso-García A, Cinco R, Gratton E (2015) Fluorescence lifetime imaging of endogenous biomarker of oxidative stress. Sci Rep 5:9848. https://doi.org/10.1038/srep09848
Datta R, Heylman C, George SC, Gratton E (2016) Label-free imaging of metabolism and oxidative stress in human induced pluripotent stem cell-derived cardiomyocytes. Biomed Opt Express 7:1690. https://doi.org/10.1364/BOE.7.001690
Datta R, Heaster TM, Sharick JT et al (2020) Fluorescence lifetime imaging microscopy: fundamentals and advances in instrumentation, analysis, and applications. J Biomed Opt 25:1. https://doi.org/10.1117/1.jbo.25.7.071203
de Oliveira FW, dos Santos Silva MP, Coelho CBBL, dos Santos Correia TM (2020) Biomarkers, biosensors and biomedicine. Curr Med Chem 27:3519–3533
Débarre D, Supatto W, Pena AM et al (2006) Imaging lipid bodies in cells and tissues using third-harmonic generation microscopy. Nat Methods 3:47–53. https://doi.org/10.1038/nmeth813
DeBerardinis RJ, Lum JJ, Hatzivassiliou G, Thompson CB (2008) The biology of cancer: metabolic reprogramming fuels cell growth and proliferation. Cell Metab 7:11–20. https://doi.org/10.1016/j.cmet.2007.10.002
DSouza AV, Lin H, Henderson ER et al (2016) Review of fluorescence guided surgery systems: identification of key performance capabilities beyond indocyanine green imaging. J Biomed Opt 21:080901. https://doi.org/10.1117/1.jbo.21.8.080901
Dvornikov A, Malacrida L, Gratton E (2019) The DIVER microscope for imaging in scattering media. Methods Protoc 2:53. https://doi.org/10.3390/mps2020053
Dysli C, Wolf S, Berezin MY et al (2017) Fluorescence lifetime imaging ophthalmoscopy. Prog Retin Eye Res 60:120–143. https://doi.org/10.1016/j.preteyeres.2017.06.005
Erkkilä MT, Bauer B, Hecker-Denschlag N et al (2019) Widefield fluorescence lifetime imaging of protoporphyrin IX for fluorescence-guided neurosurgery: an ex vivo feasibility study. J Biophotonics 12:1–8. https://doi.org/10.1002/jbio.201800378
Erkkilä MT, Reichert D, Gesperger J et al (2020) Macroscopic fluorescence-lifetime imaging of NADH and protoporphyrin IX improves the detection and grading of 5-aminolevulinic acid-stained brain tumors. Sci Rep 10:1–15. https://doi.org/10.1038/s41598-020-77268-8
Fereidouni F, Bader AN, Colonna A, Gerritsen HC (2014) Phasor analysis of multiphoton spectral images distinguishes autofluorescence components of in vivo human skin. J Biophotonics 7:589–596. https://doi.org/10.1002/jbio.201200244
Gómez CA (2018) Cerebral metabolism in a mouse model of Alzheimer's disease characterized by two-photon fluorescence lifetime microscopy of intrinsic NADH. Neurophotonics 5:1. https://doi.org/10.1117/1.nph.5.4.045008
Gosnell ME, Anwer AG, Cassano JC et al (2016) Functional hyperspectral imaging captures subtle details of cell metabolism in olfactory neurosphere cells, disease-specific models of neurodegenerative disorders. Biochim Biophys Acta - Mol Cell Res 1863:56–63. https://doi.org/10.1016/j.bbamcr.2015.09.030
Gruszecki WI, Zelent B, Leblanc RM (1990) Fluorescence of zeaxanthin and violaxanthin in aggregated forms. Chem Phys Lett 171:563–568. https://doi.org/10.1016/0009-2614(90)85264-D
Hedde PN, Cinco R, Malacrida L et al (2021) Phasor-based hyperspectral snapshot microscopy allows fast imaging of live, three-dimensional tissues for biomedical applications. Commun Biol 4:1–11. https://doi.org/10.1038/s42003-021-02266-z
Heikal AA (2010) Intracellular coenzymes as natural biomarkers for metabolic activities and mitochondrial anomalies. Biomark Med 4:241–263. https://doi.org/10.2217/bmm.10.1
Jung T, Bader N, Grune T (2007) Lipofuscin: formation, distribution, and metabolic consequences. Ann N Y Acad Sci 1119:97–111. https://doi.org/10.1196/annals.1404.008
Klemm M, Sauer L, Klee S et al (2019) Bleaching effects and fluorescence lifetime imaging ophthalmoscopy. Biomed Opt Express 10:1446. https://doi.org/10.1364/boe.10.001446
Lu H, Floris F, Rensing M, Andersson-Engels S (2020) Fluorescence spectroscopy study of protoporphyrin IX in optical tissue simulating liquid phantoms. Materials (basel) 13:7–16. https://doi.org/10.3390/ma13092105
Malacrida L, Ranjit S, Jameson DM, Gratton E (2021) The phasor plot: a universal circle to advance fluorescence lifetime analysis and interpretation. Annu Rev Biophys 50:575–593. https://doi.org/10.1146/annurev-biophys-062920-063631
Marmorstein AD, Marmorstein LY, Sakaguchi H, Hollyfield JG (2002) Spectral profiling of autofluorescence associated with lipofuscin, Bruch's membrane, and sub-RPE deposits in normal and AMD eyes. Investig Ophthalmol vis Sci 43:2435–2441
Nadiarnykh O, LaComb RB, Brewer MA, Campagnola PJ (2009) Alterations of the ECM in ovarian carcinogenesis studied by second harmonic generation imaging microscopy. Opt InfoBase Conf Pap. https://doi.org/10.1364/acp.2009.fcc1
Ostrander JH, McMahon CM, Lem S et al (2010) Optical redox ratio differentiates breast cancer cell lines based on estrogen receptor status. Cancer Res 70:4759–4766. https://doi.org/10.1158/0008-5472.CAN-09-2572
Petkovich M, Chambon P (2022) Retinoic acid receptors at 35 years. J Mol Endocrinol 69:T13–T24. https://doi.org/10.1530/JME-22-0097
Plotnikov SV, Kenny AM, Walsh SJ et al (2008) Measurement of muscle disease by quantitative second-harmonic generation imaging. J Biomed Opt 13:044018. https://doi.org/10.1117/1.2967536
Pyon WS, Gray DT, Barnes CA (2019) An alternative to dye-based approaches to remove background autofluorescence from primate brain tissue. Front Neuroanat 13:1–10. https://doi.org/10.3389/fnana.2019.00073
Ranjit S, Dvornikov A, Stakic M et al (2015) Imaging fibrosis and separating collagens using second harmonic generation and phasor approach to fluorescence lifetime imaging. Sci Rep 5:13378. https://doi.org/10.1038/srep13378
Ranjit S, Dobrinskikh E, Montford J et al (2016a) Label-free fluorescence lifetime and second harmonic generation imaging microscopy improves quantification of experimental renal fibrosis. Kidney Int 90:1123–1128. https://doi.org/10.1016/j.kint.2016.06.030
Ranjit S, Dvornikov A, Levi M et al (2016b) Characterizing fibrosis in UUO mice model using multiparametric analysis of phasor distribution from FLIM images. Biomed Opt Express 7:3519. https://doi.org/10.1364/BOE.7.003519
Ranjit SR, Dvornikov A, Dobrinskikh E et al (2017) Measuring the effect of a Western diet on liver tissue architecture by FLIM autofluorescence and harmonic generation microscopy. Biomed Opt Express 8:371–378. https://doi.org/10.1364/BOE.8.003143

Ranjit S, Datta R, Dvornikov A, Gratton E (2019a) Multicomponent analysis of phasor plot in a single pixel to calculate changes of metabolic trajectory in biological systems. J Phys Chem A 123:9865–9873. https://doi.org/10.1021/acs.jpca.9b07880

Ranjit S, Malacrida L, Stakic M, Gratton E (2019) Determination of the metabolic index using the fluorescence lifetime of free and bound nicotinamide adenine dinucleotide using the phasor approach. J Biophotonics 12:e201900156. https://doi.org/10.1002/jbio.201900156

Raub CB, Suresh V, Krasieva T et al (2007) Noninvasive assessment of collagen gel microstructure and mechanics using multiphoton microscopy. Biophys J 92:2212–2222. https://doi.org/10.1529/biophysj.106.097998

Reichert D, Erkkilae MT, Gesperger J et al (2021) Fluorescence lifetime imaging and spectroscopic co-validation for protoporphyrin IX-guided tumor visualization in neurosurgery. Front Oncol 11:1–13. https://doi.org/10.3389/fonc.2021.741303

Rich RM, Stankowska DL, Maliwal BP et al (2013) Elimination of autofluorescence background from fluorescence tissue images by use of time-gated detection and the AzaDiOxaTriAngulenium (ADOTA) fluorophore. Anal Bioanal Chem 405:2065–2075. https://doi.org/10.1007/s00216-012-6623-1

Richards-Kortum R, Sevick-Muraca E (1996) Quantitative optical spectroscopy for tissue diagnosis. Annu Rev Phys Chem 47:555–606. https://doi.org/10.1146/annurev.physchem.47.1.555

Rizou SV, Evangelou K, Myrianthopoulos V et al (2019) Correction to: a novel quantitative method for the detection of lipofuscin, the main by-product of cellular senescence, in fluids BT - cellular senescence: methods and protocols. In: Demaria M (ed) Springer. New York, NY, New York, pp C1–C2

Sachar M, Anderson KE, Ma X (2016) Protoporphyrin IX: the good, the bad, and the ugly. J Pharmacol Exp Ther 356:267–275. https://doi.org/10.1124/jpet.115.228130

Sauer L, Andersen KM, Li B et al (2018) Fluorescence lifetime imaging ophthalmoscopy (FLIO) of macular pigment. Investig Ophthalmol vis Sci 59:3094–3103. https://doi.org/10.1167/iovs.18-23886

Schweigert FJ, Siegling C, Tzimas G et al (2002) Distribution of endogenous retinoids, retinoid binding proteins (RBP, CRABPI) and nuclear retinoid X receptor β (RXRβ) in the porcine embryo. Reprod Nutr Dev 42:285–294. https://doi.org/10.1051/rnd:2002025

Seehafer SS, Pearce DA (2006) You say lipofuscin, we say ceroid: defining autofluorescent storage material. Neurobiol Aging 27:576–588. https://doi.org/10.1016/j.neurobiolaging.2005.12.006

Skala MC, Riching KM, Gendron-Fitzpatrick A et al (2007) In vivo multiphoton microscopy of NADH and FAD redox states, fluorescence lifetimes, and cellular morphology in precancerous epithelia. Proc Natl Acad Sci 104:19494–19499. https://doi.org/10.1073/pnas.0708425104

Sohal RS, Wolfe LS (1986) Lipofuscin: characteristics and significance. Prog Brain Res 70:171–183. https://doi.org/10.1016/S0079-6123(08)64304-6

Sosnik J, Zheng L, Rackauckas CV et al (2016) Noise modulation in retinoic acid signaling sharpens segmental boundaries of gene expression in the embryonic zebrafish hindbrain. Elife 5:1–14. https://doi.org/10.7554/eLife.14034

Stringari C, Cinquin A, Cinquin O et al (2011) Phasor approach to fluorescence lifetime microscopy distinguishes different metabolic states of germ cells in a live tissue. Proc Natl Acad Sci U S A 108:13582–13587. https://doi.org/10.1073/pnas.1108161108

Stringari C, Abdeladim L, Malkinson G et al (2017) Multicolor two-photon imaging of endogenous fluorophores in living tissues by wavelength mixing. Sci Rep 7:1–11. https://doi.org/10.1038/s41598-017-03359-8

Terman A, Brunk UT (2004) Lipofuscin. Int J Biochem Cell Biol 36:1400–1404. https://doi.org/10.1016/j.biocel.2003.08.009

Ung TPL, Lim S, Solinas X et al (2021) Simultaneous NAD(P)H and FAD fluorescence lifetime microscopy of long UVA–induced metabolic stress in reconstructed human skin. Sci Rep 11:1–15. https://doi.org/10.1038/s41598-021-00126-8

Warburton S, Davis WE, Southwick K et al (2007) Proteomic and phototoxic characterization of melanolipofuscin: correlation to disease and model for its origin. Mol vis 13:318–329

Weigelin B, Bakker GJ, Friedl P (2016) Third harmonic generation microscopy of cells and tissue organization. J Cell Sci 129:245–255. https://doi.org/10.1242/jcs.152272

Williams R, Chance B (1955) Respiratory enzymes in oxidative phosphorylation. III. The Steady State J Biol Chem 217:409–427. https://doi.org/10.1016/S0021-9258(19)57191-5

Yakovleva MA, Radchenko AS, Feldman TB et al (2020) Fluorescence characteristics of lipofuscin fluorophores from human retinal pigment epithelium. Photochem Photobiol Sci 19:920–930. https://doi.org/10.1039/c9pp00406h

Yan Y, Xing F, Cao J et al (2023) Fluorescence intensity and lifetime imaging of lipofuscin-like autofluorescence for label-free predicting clinical drug response in cancer. Redox Biol 59:102578. https://doi.org/10.1016/j.redox.2022.102578

Zimmermann T, Rietdorf J, Pepperkok R (2003) Spectral imaging and its applications in live cell microscopy. FEBS Lett 546:87–92. https://doi.org/10.1016/S0014-5793(03)00521-0

Zipfel WR, Williams RM, Christiet R et al (2003a) Live tissue intrinsic emission microscopy using multiphoton-excited native fluorescence and second harmonic generation. Proc Natl Acad Sci U S A 100:7075–7080. https://doi.org/10.1073/pnas.0832308100

Zipfel WR, Williams RM, Webb WW (2003b) Nonlinear magic: multiphoton microscopy in the biosciences. Nat Biotechnol 21:1369–1377. https://doi.org/10.1038/nbt899

Zong W, Wu R, Li M et al (2017) Fast high-resolution miniature two-photon microscopy for brain imaging in freely behaving mice. Nat Methods 14:713–719. https://doi.org/10.1038/nmeth.4305

Zong W, Obenhaus HA, Skytøen ER et al (2022) Large-scale two-photon calcium imaging in freely moving mice. Cell 185:1240-1256.e30. https://doi.org/10.1016/j.cell.2022.02.017

Díaz M, Malacrida L (2023) Advanced fluorescence microscopy methods to study dynamics of fluorescent proteins in vivo BT - fluorescent proteins: methods and protocols. In: Sharma M (ed). Springer US, New York, NY, pp 53–74

Friedl P, Wolf K, von Andrian UH, Harms G (2007) Biological second and third harmonic generation microscopy. Curr Protoc Cell Biol 1–21

Jung T, Höhn A, Grune T (2009) Chapter 13. B Kalilah Dimnah 594:329–330. https://doi.org/10.31826/9781463223533-017

Kalinina S, Freymueller C, Naskar N, et al (2021) Bioenergetic alterations of metabolic redox coenzymes as nadh, fad and fmn by means of fluorescence lifetime imaging techniques. Int J Mol Sci 22:. https://doi.org/10.3390/ijms22115952

Leemans S, Dvornikov A, Gallagher T, Gratton E (2020) AO DIVER: development of a three-dimensional adaptive optics system to advance the depth limits of multiphoton imaging. APL Photonics 5:. https://doi.org/10.1063/5.0032621

Liu Z, Pouli D, Alonzo CA, et al (2018) Mapping metabolic changes by noninvasive, multiparametric, high-resolution imaging using endogenous contrast. Sci Adv 4:. https://doi.org/10.1126/sciadv.aap9302

Ma N, Digman MA, Malacrida L, Gratton E (2016) Measurements of absolute concentrations of NADH in cells using the phasor FLIM method. Biomed Opt Express 7:. https://doi.org/10.1364/BOE.7.002441

Ranjit S, Malacrida L, Jameson DM, Gratton E (2018) Fit-free analysis of fluorescence lifetime imaging data using the phasor approach. Nat Protoc 1. https://doi.org/10.1038/s41596-018-0026-5

Stringari C, Nourse JL, Flanagan LA, Gratton E (2012) Phasor fluorescence lifetime microscopy of free and protein-bound NADH reveals neural stem cell differentiation potential. Plos One 7:. https://doi.org/10.1371/journal.pone.0048014

Torrado B, Malacrida L, Ranjit S (2022) Linear combination properties of the phasor space in fluorescence imaging. Sensors 22:. https://doi.org/10.3390/s22030999

Tserevelakis GJ, Megalou E V., Filippidis G, et al (2014) Label-free imaging of lipid depositions in C. elegans using third-harmonic generation microscopy. Plos One 9:. https://doi.org/10.1371/journal.pone.0084431

Yildirim M, Sugihara H, So PTC, Sur M (2019) Functional imaging of visual cortical layers and subplate in awake mice with optimized three-photon microscopy. Nat Commun 10:. https://doi.org/10.1038/s41467-018-08179-6